BNL-226235-2024-TECH
C-A/AP/712

Measuring Magnets Transfer Functions in the NSRL Transport Line

B. Dhital

October 2024

Collider Accelerator Department
Brookhaven National Laboratory

U.S. Department of Energy
USDOE Office of Science (SC), Nuclear Physics (NP)

DISCLAIMER

Measuring Magnets Transfer Functions in the NSRL Transport Line

Bhawin Dhital, Petra Adams, Kevin Brown, Trevor Olsen,
Michael Sivertz & Nicholaos Tsoupas
Brookhaven National Laboratory, Upton NY 11973
Lucy Lin
Cornell University, Ithaca, New York 14853, USA

Abstract

The beamline at the NASA Space Radiation Laboratory (NSRL) is equipped with a range of magnets, including dipole magnets, dipole corrector magnets, quadrupole magnets, sextupole magnets, and octupole magnets. The magnet transfer function defines the relationship between the power supply currents and the corresponding magnet strengths. This note presents the measurements of the transfer functions for the dipole correctors and quadrupole magnet in the NSRL beamline.

1 Introduction

As illustrated in Fig. 1, The beamline comprises three dipole magnets forming a 20° bends, nine quadrupole magnets (Q1–Q9), and two octupole magnets (Oct1 and Oct2). The octupole magnets are positioned upstream of Q5 and Q6, respectively, and are adjustable to achieve a uniform rectangular beam distribution on the target [1, 2]. The optical design of the beamline ensures an achromatic beam following the 20° dipole bend, which is essential for maintaining beam uniformity as momentum-dependent motion at the octupole entrances can affect distribution uniformity. Upon traversing the foil, the transverse phase space distribution of the beam transforms into a Gaussian

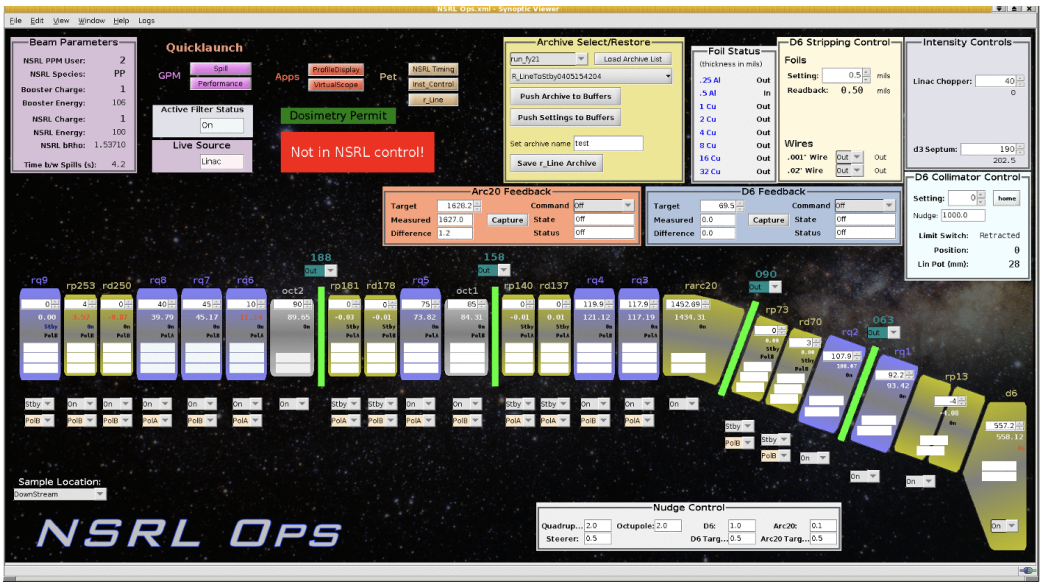

Figure 1: NSRL beamline with different magnet and current set up in the operational mode.

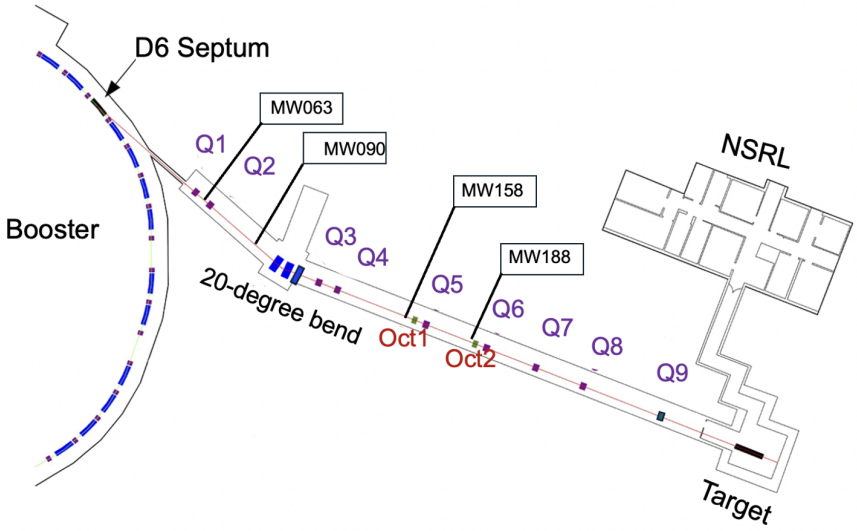

Figure 2: Schematic drawing of the NSRL beamline showing different magnet components and SWICs.

distribution at the entrance of the D6 septum [3, 4]. This Gaussian distribution, after passing through the various magnets along the NSRL beamline, facilitates the generation of uniform beam distributions at the NSRL target [1], which is critical for the success of various beam experiments.

Additionally, a set of dipole correctors is installed along the NSRL beamline. The horizontal dipole correctors, designated as RD70, RD137, RD178, and RD250, and the vertical dipole correctors, designated as RP13, RP73, RP140, RP181, and RP253, respectively, serve to center the beam in the horizontal and vertical planes. To achieve this centering, specific currents, typically on the order of a few amperes, are supplied to these corrector magnets. The relationship between the applied currents and the resulting magnetic fields of these correctors is critical for defining their strengths. Therefore, it is necessary to characterize the magnetic field response to various current values to precisely determine the corrector strengths.

To establish a precise correlation between currents and the magnetic field strengths of the NASA Space Radiation Laboratory (NSRL) beamline magnets, it is essential to define a transfer function for each magnet type. This note outlines a detailed experimental methodology for determining the magnetic field strengths of the dipole corrector and quadrupole magnets.

2 Transfer Function

The transfer function is defined by [5]

$$\begin{array}{ll} BL/I & [\text{Tm/A}] \quad \text{for a dipole} \\ GL/I & [\text{T/A}] \quad \text{for a quadrupole,} \end{array} \tag{1}$$

where B and G are the dipole magnetic field and quadrupole gradient respectively. L is the length of the magnet and I is the current in amps. In principle, magnet transfer function is ideally constant. However in reality this may not be true because of saturation of current.

Let us consider the following derivation starting from Lorentz force equation,

$$F = \frac{dp}{dt} = q(E + V \times B), \tag{2}$$

where symbols have their usual meanings and F, p, E, V, and B are vectors. Let us consider the dipole magnet which bends the beam trajectory by angle

θ. Then Eq. 2 can be written as

$$\begin{aligned} \frac{dp}{dt} &= p_0 \frac{d\theta}{dt} \\ &= p_0 \frac{d\theta}{ds} \cdot \frac{ds}{dt} \\ qv_z B &= p_0 \frac{d\theta}{ds} \cdot v_z \\ \Delta\theta &= \frac{BL}{B\rho}; ds = L, B\rho = p_0/q. \end{aligned} \tag{3}$$

Now the dipole magnet transfer function is obtained as

$$\frac{BL}{I} = \frac{\Delta\theta}{\Delta I} \cdot B\rho \tag{4}$$

For quadrupole magnet, $\Delta\theta$ is defined by the quadrupole field strength k,

$$\begin{aligned} \Delta\theta = \frac{x}{1/k} = kx = \frac{BL}{B\rho} &= \frac{GxL}{B\rho} \\ GL &= k \cdot B\rho \\ \frac{GL}{I} &= B\rho \cdot \frac{\Delta k}{\Delta I} \end{aligned} \tag{5}$$

Eq. (4) and Eq. (5) will be used to calculate the dipole manget and quadrupole magnet transfer functions from the beam measurements.

2.1 Transfer function for vertical correctors

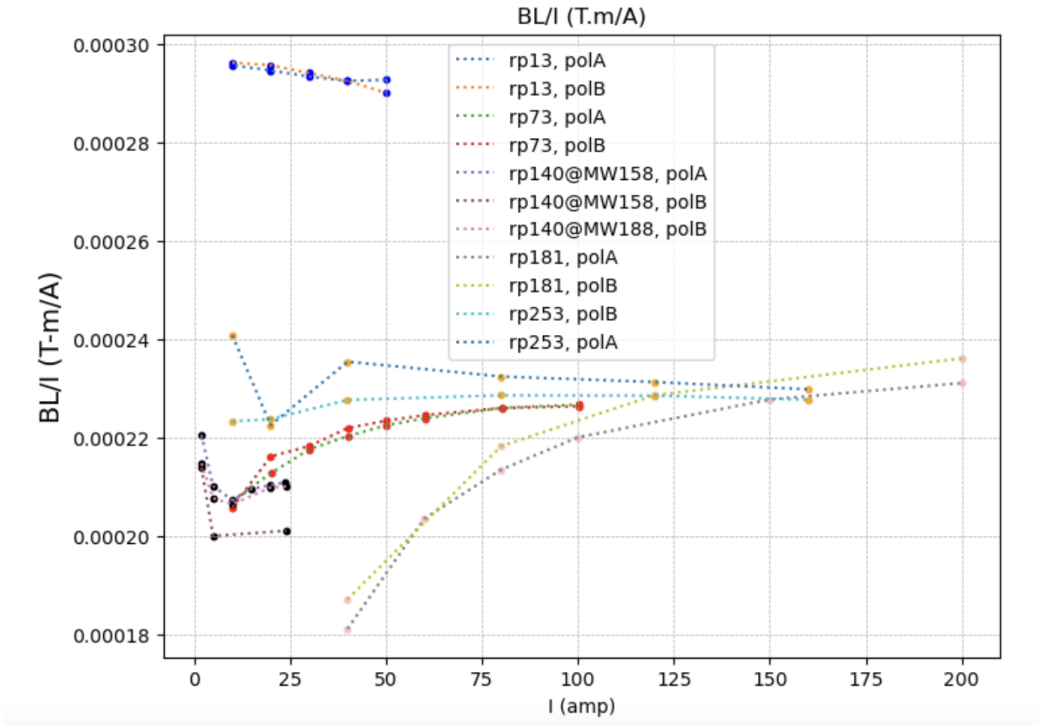

Figure 3: BL/I versus I plot for all vertical correctors. At higher current value, all vertical corrector magnets transfer function converges to about 0.00023 (T-m/A), except for rp13 corrector. This is explained in section 4.

2.2 Transfer function for horizontal correctors

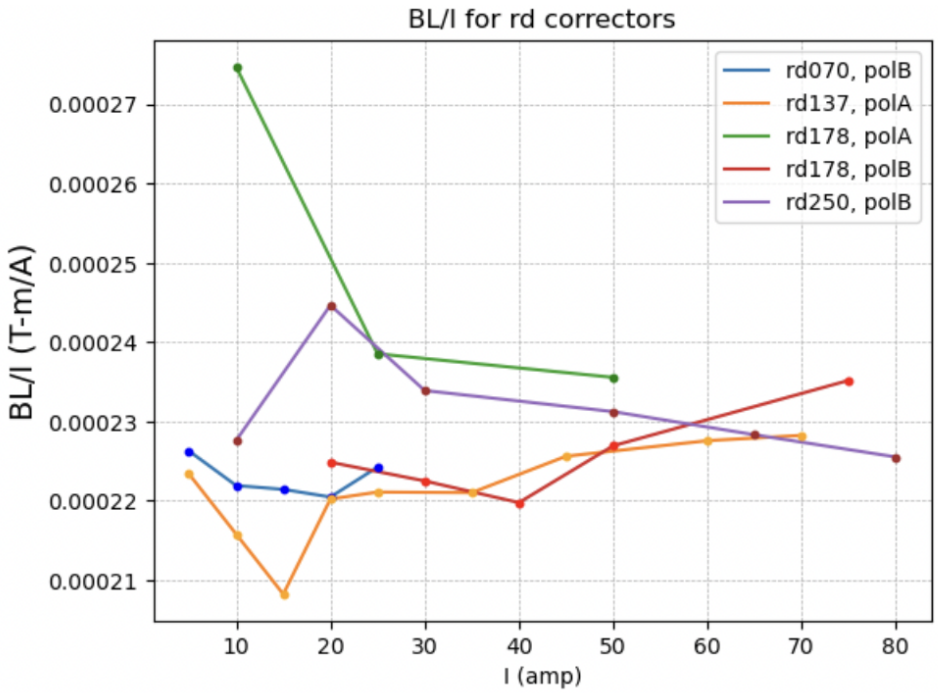

Figure 4: BL/I versus I plot for all horizontal correctors. At higher current, all horizontal correctors transfer function converges to about 0.00023 (T-m/A).

3 Quadrupole Magnets Transfer Function

There are 9 quadrupole magnets in the NSRL beam line. The distance between the quadrupoles and the corresponding multi-wires location in the beamline is presented in Table 3. Figure 5 shows the rQ1 quadrupole transfer function measured with beam profile displacement at multi-wire MW063 and MW090 respectively. The value of the quadrupole transfer function is about 0.0057 T/m. The details on the procedure to calculate the quadrupole transfer function including a model for one-turn transfer map is presented in Appendix. C.2.

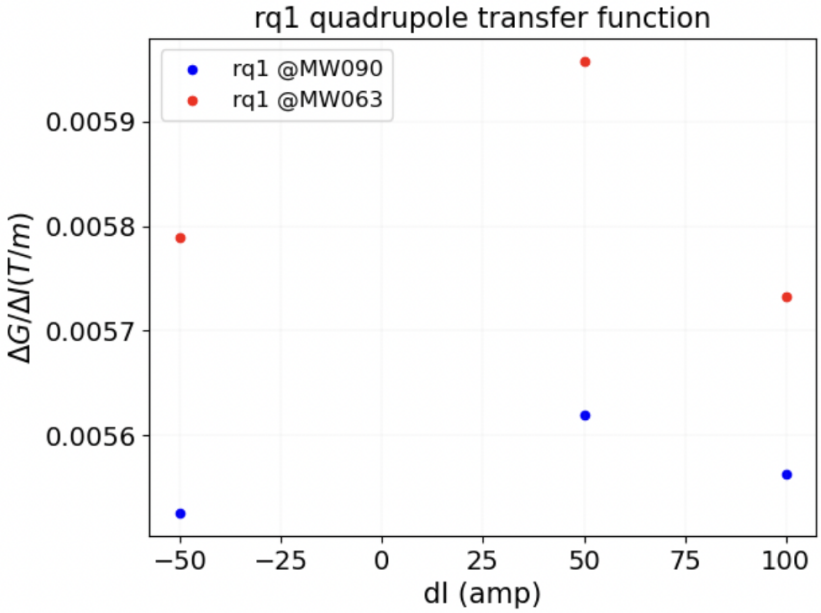

Figure 5: Transfer function for rq1 quadrupole

All quadrupoles in the NSRL beamline are the same and they should have the same transfer function as the first quadrupole rQ1. Due to a limit to the experimental time available for the beam experiment, we are unable to measure all quadrupoles transfer function at this point.

4 Result and Discussion

We measured the transfer function of all five vertical correctors (RP13, RP73, RP140, RP181, and RP253) and all four horizontal correctors (RD70, RD137, RD178, and RD250) in the NSRL beamline, following the experimental procedure outlined in the previous section. We utilized Silicon ions with a kinetic energy of 613.85 MeV per nucleon at the beginning of the NSRL beamline. The rigidity $B\rho = 8$ T-m for Q = 14, and $\beta * \gamma = 1.38$.

The mean value of the transfer function for RP13 was approximately 0.00029 T-m/A. For all other correctors, the transfer function values converged close to 0.00023 T-m/A at higher currents, as illustrated in Fig. 3.

Notably, the total length, aperture and number of turns of RP13 and other vertical correctors differed. While RP13 had a total length of 2 $\times$ 0.2032 m, the other vertical correctors shared a total length of 2×0.31496 m. Additionally, RP13 had a magnet aperture of 5 inches, whereas other correctors had an aperture of 8 inches. We approximated the relationship as follows:

$$\frac{BLI_{rp13}}{BLI_{rp73}} = \frac{L_{rp13}}{L_{rp73}} \times \frac{Aper_{rp73}}{Aper_{rp13}} \times \frac{N_{rp73}}{N_{rp13}} = \frac{0.00029}{0.00023} \approx 1.3. \tag{6}$$

From the above relationship, we get the following relationship between the number of turns of coils in rp13 and rd73 as

$$\frac{N_{rp73}}{N_{rp13}} \approx 1.25. \tag{7}$$

BNL archive document shows that there are 32 turns per coil in all dipoles in the beam line except rp13. If it is true, to meet the ratio of number of coils defined in Eq. (7), $N_{rp13} \approx 25$.

On average all horizontal and vertical correcotrs transfer function is about 0.00023 T-m/A except for rp13 which has a value of about 0.00029 T-m/A due to different physical dimensions and the number of turns in the coil of the magnet. Quadrupole magnet transfer function from the measurement is about 0.0057 (T/A).

5 Acknowledgment

The authors would like to thank Vincent Schoefer at Collider Accelerator Department at BNL for the valuable discussions on quadrupole transfer function

measurements.

A Multi-wire

To measure the beam profile along the NSRL beamline, multi-wires, also referred to as Segmented Wire Ion Chambers (SWICs), are positioned at various locations. The NSRL beamline includes five multi-wires (with four shown in Fig. 1). These multi-wires measure both horizontal and vertical beam profiles, with each plane consisting of 32 equally spaced wires. The spacing of these wires is utilized when fitting the profile of a Gaussian beam at the corresponding multi-wire location using the following algorithm.

```
#odd spacing example
num = 32
spacing_x = 1.5
xstart = -((num / 2) * spacing_x)
if num % 2 == 0:
    xstart += (spacing_x / 2)
x = xstart + np.arange(num) * spacing_x
x
array([-23.25, -21.75, -20.25, -18.75, -17.25, -15.75, -14.25, -12.75,
       -11.25,  -9.75,  -8.25,  -6.75,  -5.25,  -3.75,  -2.25,  -0.75,
         0.75,   2.25,   3.75,   5.25,   6.75,   8.25,   9.75,  11.25,
        12.75,  14.25,  15.75,  17.25,  18.75,  20.25,  21.75,  23.25])
#Even spacing example
num = 32
spacing_x = 6.0
xstart = -((num / 2) * spacing_x)
if num % 2 == 0:
    xstart += (spacing_x / 2)
x = xstart + np.arange(num) * spacing_x
x
array([-93., -87., -81., -75., -69., -63., -57., -51., -45., -39., -33.,
       -27., -21., -15.,  -9.,  -3.,   3.,   9.,  15.,  21.,  27.,  33.,
        39.,  45.,  51.,  57.,  63.,  69.,  75.,  81.,  87.,  93.])
```

The array represents the Gaussian profile length in mm, equally spaced from the center.

Multi-wire	X spacing (mm)	Y spacing (mm)
MW063	6.0	6.0
MW090	1.5	6.0
MW158	6.0	1.5
MW188	3.0	6.0
MW302	12.0	12.0

Table 1: Different multi-wire spacing in the NSRL.

B Magnets distance from multi-wires

B.1 Dipole corrector magnets from the multi-wires

Table 2: Distance between dipole corrector magnets and the multi-wires.

rp13	distance from SWIC063	15.0346917 m
rd70	distance from SWIC090	7.756 m
rp73	distance from SWIC090	6.8416
rd137	distance from SWIC158	8.9144 m
rp140	distance from SWIC158	8.0 m
rp140	distance from SWIC188	16.44 m
rd178	distance from SWIC188	4.9144 m
rp181	distance from SWIC188	4.0 m
rd250	distance from SWIC302	16.9144 m
rd250	distance from SWIC302	16.0 m

B.2 Quadrupole magnets from the multi-wires

Table 3: Distance between quadrupoles and the multi-wires.

rq1	distance from SWIC063	1.0 m
rq2	distance from SWIC090	8.90926 m
rq3	distance from SWIC158	12.67706 m
rq4	distance from SWIC158	10.09306 m
rq5	distance from SWIC188	6.09306 m

C Experimental Procedure

C.1 Dipole corrector transfer function

The following setup was used in our experiment:

- All magnets, except the one for which the transfer function is being measured, are turned off (set to stand-by mode).
- The current in the magnet is varied from an initial value to a final value within the operational limits.
- For each current value, the corresponding beam profiles are recorded using the first multi-wire detector located immediately downstream of the magnet. For example, when varying currents in the RP13 corrector, the beam profile is observed at the multi-wire MW063 location for the various current settings.
- As the current varies, the beam profile shifts in the observed multi-wire.
- This process is repeated for each dipole corrector magnet.

Figure 6 illustrates the beam profile displacement at the multi-wire resulting from the variation in current applied to the magnet. Let θ be the angle by which the beam deviates passing through the magnet, and the beam profile displaces by Δx m as shown in Fig 6. The approximate relationship between the angle θ and the displacement Δx is given by

$$\Delta\theta = \frac{\Delta x}{L}, \tag{8}$$

where L is the distance between magnet and the multi-wire location along

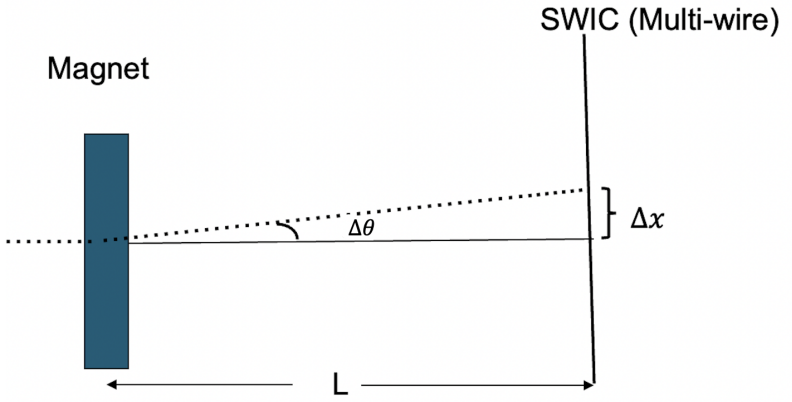

Figure 6: Beam profile displacement at the multi-wire resulting from the variation in current applied to the magnet.

the beamline. Furthermore, in terms of the magnetic field B and the ring radius ρ, the angle θ can be expressed as

$$\frac{Bl}{B\rho} = \Delta\theta = \frac{\Delta x}{L} \quad \text{from Eq. (4)}, \tag{9}$$

where l is the magnet length. The beam rigidity $B\rho$ for the given ion species is defined by [6]

$$B\rho = k\left(\frac{mc^2}{Q}\right)\beta\gamma, \tag{10}$$

where $k = 10^9/c$, mc^2 is the rest mass energy given in GeV/c and $\beta\gamma$ are the relativistic energy factor,and c is the speed of light in vacuum respectively. Hence, for each profile displacement corresponding to a specific current value I, the quantity Bl/I can be calculated.

C.2 Quadrupole magnet transfer function

Under thin lens approximation, We vary rp13 corrector currents to -25,-50, 0 amps and rq1 quadrupole currents to 300, 350, and 250 amps respectively. Taking one -turn transfer map starting at rp13 to the multi-wire location MW063, one can write in Mathematica using thin lens approximation:

```
Q1 = {{1, 0}, {k1, 1}};
Q2 = {{1, 0}, {k2, 1}};
D1 = {{1, d1}, {0, 1}};
D2 = {{1, d2}, {0, 1}};
```

where $k1$ and $k2$ are the quadrupole strengths for different current values, $d1$ and $d2$ are drift between MW063 and rq1 and between rp13 and rq1 respectively. We assume the rp13 corrector is at a constant current which gives kick θ. Let us suppose the initial position and angle be $(x0, xp0)$, then we write in the matrix form:

```
v0 = {{x0}, {xp0}};
```

```
vc = {{x0},{xp0+θ};
```

Now one-turn transfer map starting from rp13 corrector to the multi-wire MW063 for one value of quadrupole current can be written as

$$M1 = D1.Q1.D2 \tag{11}$$

Similarly, for the same rp13 corrector setting and for different quadrupole current setting, the one-turn transfer map becomes

$$M2 = D1.Q2.D2 \tag{12}$$

Then,

```
    vf1 = M1 . vc
    (1 + d1 k1) x0 + (d1 + d2 (1 + d1 k1)) (xp0+θ), k1 x0 + (1 +
      d2 k1) ((xp0+θ)
```

```
vf2 = M2 . vc
(1 + d1 k2) x0 + (d1 +
      d2 (1 + d1 k2)) (xp0+θ), k2 x0 + (1 +
      d2 k2) (xp0+θ)
```

We observe dx in the multi-wire MW063 for each case and match it in the model.

```
dx = vf2[[1, 1]] - vf1[[1, 1]]
```

And simplifying, we ger

dx = -d1 (k1 - k2) (x0 + d2 (xp0+θ).

For two values of quadrupole strengths and two different rp13 settings, we can write two equations as

$$\frac{dx_1}{-d_1(k_1 - k_2)} = (x_0 + d_2(xp_0 + \theta_1)) \tag{13}$$

$$\frac{dx_2}{-d_1(k_1 - k_2)} = (x_0 + d_2(xp_0 + \theta_2)) \tag{14}$$

Subtracting the above two equations,

$$\Delta k = \frac{(\Delta x)_1 - (\Delta x)_2}{d_1 d_2(\theta_1 - \theta_2)}; \quad \Delta k = (k_2 - k_1) \tag{15}$$

Since $\Delta k/\Delta I = \Delta k/\Delta x.\Delta x/\Delta I$. Dividing the above Eq. (15) by ΔI gives

$$\frac{\Delta k}{\Delta I} = \frac{(\Delta x)_1 - (\Delta x)_2}{\Delta I d_1 d_2(\theta_1 - \theta_2)}; \quad \Delta k = (k_2 - k_1) \tag{16}$$

This gives the change in quadrupole strength with the change in the quadrupole currents.

D Error Analysis

From Eq. (8), we can write

$$\Delta\theta = \frac{\Delta x}{L}, \tag{17}$$

and $\Delta\theta$ is a function of a power supplies current I defined as

$$\Delta\theta = CdI, \tag{18}$$

where C is the calibration constant. Combining Eq. (17) and Eq. (18), we can write,

$$C = \frac{\Delta x}{LdI}. \tag{19}$$

It shows that C is a function of independent variables x, L and I. If we assume that the uncertainties are relatively small, then we add the errors as [7]

$$\begin{aligned}(\Delta C)^2 = &\left(\frac{\partial C(\Delta x, L, dI)}{\partial(\Delta x)}\Delta(\Delta x)\right)^2 + \quad \left(\frac{\partial C(\Delta x, L, dI)}{\partial L}\Delta L\right)^2 + \\ &\left(\frac{\partial C(\Delta x, L, dI)}{\partial(dI)}\Delta(dI)\right)^2.\end{aligned} \tag{20}$$

$\Delta x = x - x_0$, where x is the centroid of the Gaussian beam profile and x_0 is the centroid of the reference Gaussian beam profile for 0 A power supply current. The uncertainty in Δx is calculated as

$$\Delta(\Delta x)^2 = (\Delta x)^2 + (\Delta x_0)^2. \tag{21}$$

Since L is the fixed distance between the magnet of consideration and the multi-wire along the beam line, we consider L as a fixed parameter. Hence Eq. (20) takes the form:

$$(\Delta C)^2 = \left(\frac{\partial C(\Delta x, L, dI)}{\partial(\Delta x)}\Delta(\Delta x)\right)^2 + \quad \left(\frac{\partial C(\Delta x, L, dI)}{\partial(dI)}\Delta(dI)\right)^2. \tag{22}$$

In our studies, we are taking a fixed power supplies set points. It means, all uncertainties basically arise from beam profile measurement. Hence error on the calibration constant C can be written as

$$(\Delta C)^2 = \left(\frac{\partial C(\Delta x, L, dI)}{\partial(\Delta x)}\Delta(\Delta x)\right)^2. \tag{23}$$

References

[1] N Tsoupas et al. "Uniform particle beam distributions produced by octupole focusing". In: *Nuclear science and engineering* 126.1 (1997), pp. 71–79. URL: https://www.tandfonline.com/doi/abs/10.13182/NSE97-A24458.

[2] Nicholaos Tsoupas et al. "Results from the Commissioning of the NSRL Beam Transfer Line at BNL". In: *Proceedings of the 2004 European Particle Accelerator Conference, Luzern*. 2004. URL: https://accelconf.web.cern.ch/e04/PAPERS/THPLT183.PDF.

[3] Bhawin Dhital et al. *Beam Scattering Through Foil at NSRL*. Tech. rep. Brookhaven National Laboratory (BNL), Upton, NY (United States), 2024. URL: https://www.osti.gov/servlets/purl/2336584/.

[4] B. Dhital et al. "Bmad based particle tracking simulation for slow resonant extraction". In: *Proc. 15th International Particle Accelerator Conference* (Nashville, TN). JACoW Publishing, Geneva, Switzerland, May 2024, pp. 1164–1167. ISBN: 978-3-95450-247-9. DOI: 10.18429/JACoW-IPAC2024-TUPC69. URL: https://indico.jacow.org/event/63/contributions/3780.

[5] Fulvia Pilat. *ATR Magnet Transfer Functions*. Tech. rep. Brookhaven National Lab.(BNL), Upton, NY (United States), 1995. URL: https://www.bnl.gov/isd/documents/82915.pdf.

[6] Christopher Gardner. *Notes on calculating various parameters of ions circulating in Booster and destined for NSRL*. Tech. rep. Brookhaven National Lab.(BNL), Upton, NY (United States), 2019. URL: https://www.osti.gov/servlets/purl/1545591/.

[7] John Robert Taylor and William Thompson. *An introduction to error analysis: the study of uncertainties in physical measurements*. Vol. 2. Springer, 1982.

[8] K Brown et al. "Design of a resonant extraction system for the AGS booster". In: *Proceedings of the 1999 Particle Accelerator Conference (Cat. No. 99CH36366)*. Vol. 2. IEEE. 1999, pp. 1270–1272. URL: https://ieeexplore.ieee.org/abstract/document/795518.